BIOLOGICAL CONTROL

A Regional Analysis of Weather Mediated Competition Between a Parasitoid and a Coccinellid Predator of Oleander Scale

Andrew P. Gutierrez[1,2] and Marina A. Pizzamiglio[1,3]

[1]*College of Natural Resources, Division of Ecosystems Science, University of California, Berkeley, CA, 94706, USA*
[2]*Center for the Analysis of Sustainable Agricultural Systems (CASAS), Kensington, CA, 94707, USA*
[3]*Former address: Instituto Agronômico do Paraná, Londrina, PR, Brazil*

Neotropical Entomology 36(1):070-083 (2007)

Análise Regional da Competição Mediada por Fatores Climáticos entre um Parasitóide e um Coccinelídeo Predador da Cochonilha-da-Espirradeira na Califórnia

RESUMO - O controle natural de uma população assexuada de cochonilha-da-espirradeira (*Aspidiotus nerii* Bouchè (Hemiptera: Diaspididae) em plantas do louro da California [*Umbellularia californica* (Hopk. & Arn.) Nut.] por dois de seus inimigos naturais [*Aphytis chilensis* Howard (Hymenoptera: Aphelinidae) e *Rhysobius lophanthae* (Blaisd.) (Coleoptera: Coccinellidae)] foi examinado em meio-ambiente com mudanças climáticas usando um modelo geral tritrófico, com base em estrutura populacional de idade e massa e acionado por condições climáticas. O modelo é de complexidade intermediária e os parâmetros foram obtidos através de extensas observações de laboratório e campo em Albany, Califórnia. Índices fisiológicos dependentes de temperatura foram desenvolvidos a partir de dados de laboratório e usados para modificar o crescimento per capita, fecundidade e taxas de sobrevivência dos valores máximos. O modelo tritrófico foi integrado em GIS (sistema geográfico de informação) e a dinâmica das espécies foi examinada através dos anos e das zonas ecológicas da Califórnia. Dados de campo e resultados de modelagem sugerem que o coccinelídeo predador é o agente mais importante no controle da cochonilha-da-espirradeira no clima ameno de Albany. Entretanto, a análise de regressão linear multivariada de dados de simulações regionais, demonstra que, sob altas temperaturas, *A. chilensis* é o fator mais importante suprimindo as densidades da cochonilha, enquanto o predador *R. lophanthae* é mais eficiente em regiões mais frias. A presença de *R. lophanthae* aumenta a densidade da cochonilha 9,7% em média através das zonas ecológicas da Califórnia.

PALAVRAS-CHAVE: GIS, dinâmica de população, oliveira, modelo com base fisiológica

ABSTRACT - The regulation of an asexual population of the oleander scale [*Aspidiotus nerii* Bouchè (Hemiptera: Diaspididae)] on California bay tree [*Umbellularia californica* (Hopk. & Arn.) Nut.] by two natural enemies; an idiobiont, ectoparasitoid *Aphytis chilensis* Howard (Hymenoptera: Aphelinidae) and a coccinellid predator (*Rhysobius lophanthae* (Blaisd.) (Coleoptera: Coccinellidae), was examined using a general weather-driven, tri-trophic, physiologically based age-mass structured demographic model. The model is of intermediate complexity and was parameterized using extensive laboratory data and field observations from Albany, CA. Temperature-dependent physiological indices were estimated from the laboratory data and used to scale per capita growth, fecundity and survivorship rates from maximal values in a time varying environment. The tri-trophic model was integrated in a GIS (geographic information system) and the species dynamics examined across years and across the ecological zones of California. Field data and simulation results suggested the coccinellid predator was the most important regulating agent of oleander scale in the mild climate of Albany. However, multiple linear regression analysis of simulation data across all ecological zones of California shows that the parasitoid *A. chilensis* is the most important agent in suppressing oleander scale densities in warmer climates, while the predator *R. lophanthae* increases scale density an average of 9.7% across all regions.

KEY WORDS: GIS, population dynamics, olive, physiologically based model

The distribution and regulation of poikilotherm populations by natural enemies are greatly influenced by weather (Andrewartha & Birch 1954, Huffaker *et al*. 1971). The dynamics of the same species and the level of regulation may vary considerably under different weather regimes (Rochat & Gutierrez 2001). Models are commonly used to examine predator-prey systems, but failure to incorporate the weather driven biology of the species has often obscured the underlying mechanisms of population regulation and this has contributed to controversy (Hughes & Gilbert 1968, Gilbert & Gutierrez 1973, Gilbert *et al*. 1976, Lawton 1977).

Simplification of models that ignore weather effects are often made because of the well known tradeoffs between the benefits of increased realism and the lessened mathematical tractability and hinder analysis of model stability and other attributes (see Wang & Gutierrez 1980, Godfray & Waage 1991). In this paper, we chose the path of increased realism to examine the effects of weather on the regulation of an asexual population of oleander scale [*Aspidiotus nerii* Bouchè (Hemiptera: Diaspididae)] on California bay tree [*Umbellularia californica* (Hopk. & Arn.) Nut.] by a thelytokous, idiobiont, ectoparasitoid *Aphytis chilensis* Howard (Hymenoptera: Aphelinidae) and a coccinellid predator [*Rhysobius lophanthae* (Blaisd) (Coleoptera: Coccinellidae)] (see Gutierrez & Baumgärtner 1984). None of these species has a dormant period. Oleander scale is also a pest of olive (*Olea europaea* L.) (Ferris 1938), and this was a major motivation for our study. Specifically, the study sought to estimate the relative contribution of the two natural enemies in the control of oleander scale in a time varying environment, and secondly to illustrate the separate effects of weather on control across the ecological areas of California favorable for olive production.

A weather driven, physiologically based, age-mass structured model of the interactions of the four species was developed and used to evaluate the system's dynamics. Unless indicated, the extensive laboratory and field data on *A. nerii* and *A. chilensis* (Pizzamiglio 1985) and laboratory data on *R. lophanthae* (Cividanes & Gutierrez 1996) were used to parameterize the model (Figs. 1-3). All of the data were collected at Albany, California on the eastern shore of San Francisco Bay. The numerical predictions of the model are compared qualitatively to field data reported by Pizzamiglio (1985), and the stability properties of the model were analyzed graphically. The model was integrated into a geographic information system (GIS) to map and analyze the simulation data from 108 locations across the ecological zones of California.

Biology of the species

Bay tree. Bay tree is evergreen with growth being greatest in spring, though growth may occur year around. Photosynthesis was modeled to estimate tree mass growth rates and to capture its bottom-up effects on oleander scale populations. A more detailed model for olive was also used in the study (see Gutierrez *et al*. 2006).

Oleander scale. *A. nerii* is a cosmopolitan species that occurs as distinct asexual and sexual populations (DeBach & Fisher 1956). It feeds on leaves, bark and fruits on a wide range of host plants including olive (Ferris 1938). As in all Coccoidea, the asexual females of the California population are neotenic (i.e. morphologically a larva, with a soft round body concealed under the scale cover or carapace). The scale is oviparous and lays its eggs under its hard carapace where incubation and eclosion occur. After eclosion, the first instar larvae (i.e. crawlers) escape from the carapace and wander for a short period before settling (i.e. the white cap stage) to remain sessile for the rest of their lives. Post-embryonic

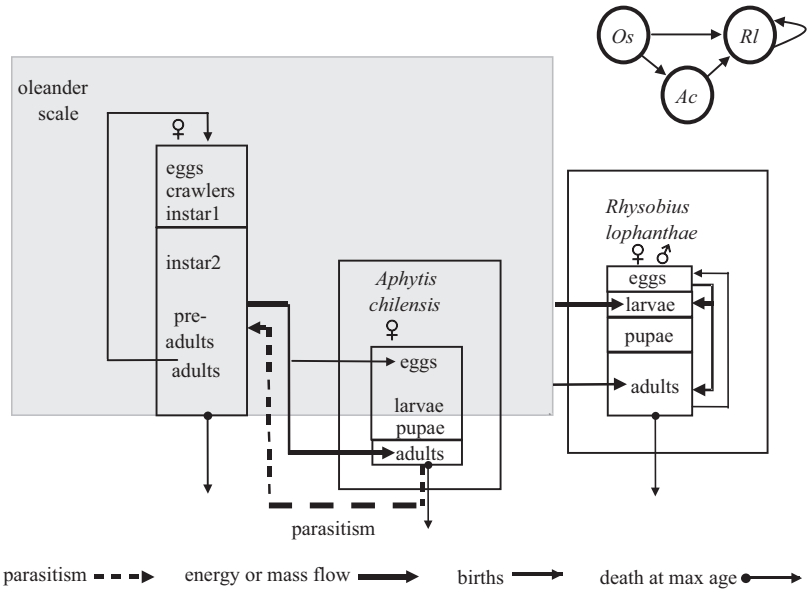

Fig. 1. The biological interactions of the oleanders scale, the parasitoid *A. chilensis,* and the coccinellid predator *R. lophanthae*.

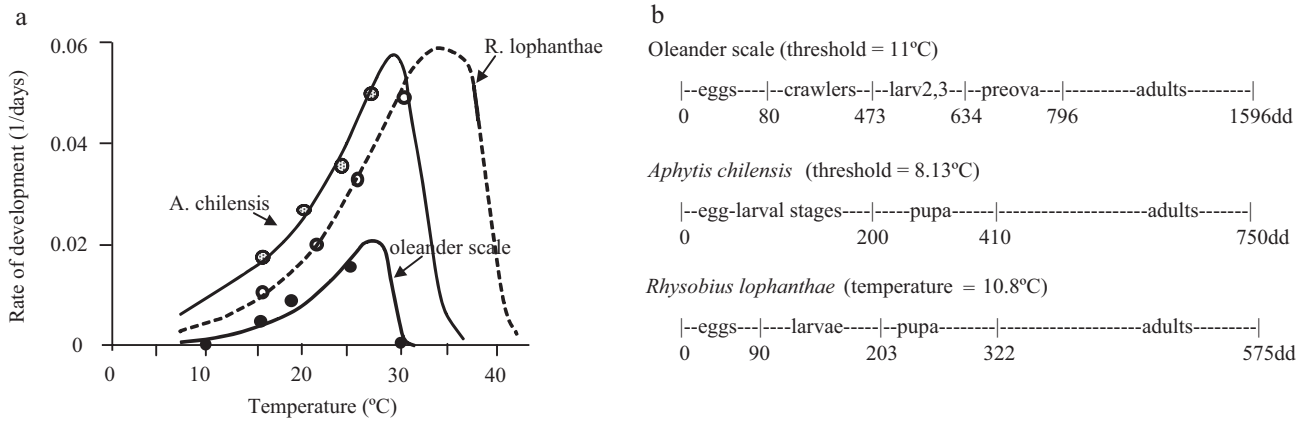

Fig. 2. The effect of temperature on the developmental rates of (a) oleander scale, *A. chilensis* and *R. lophanthae*, and (b) the developmental times in degree-days of the life stages of the three species.

development in this scale consists of three instars in females and five instars in males of sexual populations.

A. chilensis. All species of the genus *Aphytis* are parasitoids of armored scales with *A. chilensis* being the type species (Rosen & DeBach 1979). All adults are females that prefer to attack late second instar and young adult scale. At 20ºC, a female may parasitize nine scales per day and host feeds on an additional 14.4 scales (i.e. 1:1.6). The adult parasitoid pierces the scale carapace with its ovipositor and lays one or more eggs externally on the surface of the scale larvae where the parasitoid larva feeds and pupates. Only one parasitoid matures per scale. The egg-to-egg period of the parasitoid is half that of the scale.

R. lophanthae. This coccinellid species is native to Australia and South Africa (Gordon 1985) and has been introduced widely for control of armored scale. Adult females deposit their eggs under the carapace of dead scales or near live prey (DeBach 1964). The egg-to-egg period of the predator is 3/8 that of the scale resulting in 2.6 beetle generations per scale generation. At 25ºC, a newly hatched *R. lophanthae* larvae consumes 100 third instar scale (i.e. 5.6mg dry weight) to reach maturity. An adult female may consume 100-125 large scales during the adult period, and an adult male may consume half that number. On average, 20 eggs d^{-1} are produced per 8-9 large scales consumed d^{-1}. Coccinellid larvae and adults also attack parasitized scale and increasingly cannibalize their own eggs and larvae as scale prey become scarce.

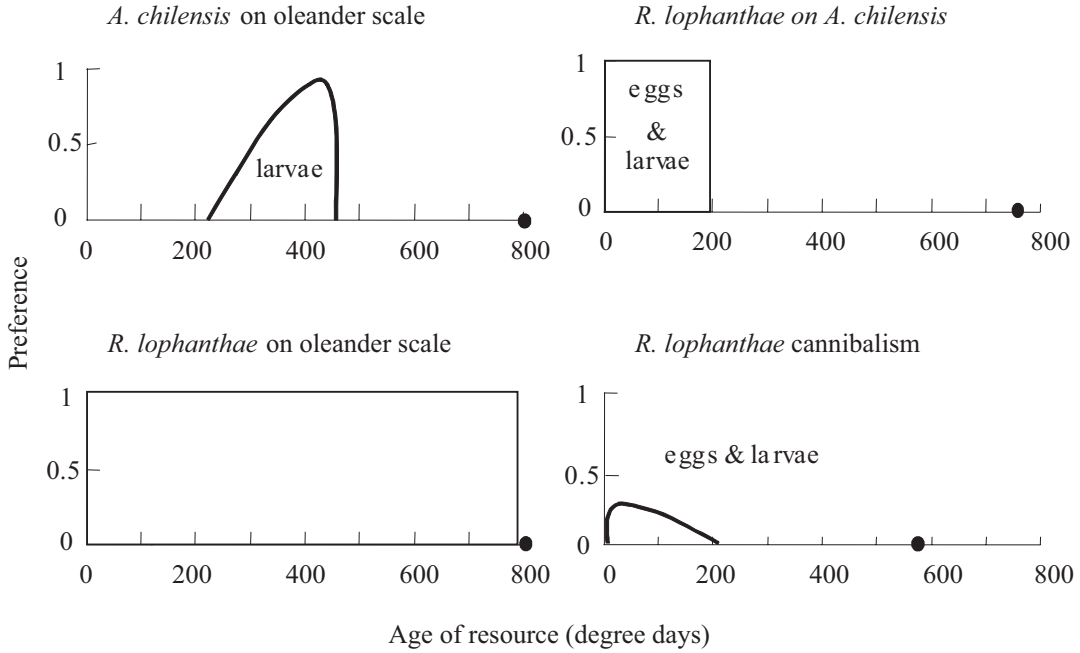

Fig. 3. Preference relationships: (a) *A. chilensis* for oleander scale life stages, and *R. lophanthae* preferences for (b) oleander scale, (c) *A. chilensis* and (d) its own life stages.

R. lophanthae is the most numerous predator of *A. nerii* in Greece, but is thought to play a subsidiary role to the parasitoid *A. chilensis* in regulating pest scales (Argyriou & Kourmadas 1980). In contrast, *R. lophanthae* was found to be the most important natural enemy of *A. nerii* in California (Pizzamiglio 1985).

The model. The mathematics of the physiologically based model is reviewed in the appendix and in the references therein. Here only the basic details are outlined.

Basic assumptions of the model include: (1) all species including plants are predators in a general sense, (2) the resource acquisition rate (i.e. a type III functional response) is the death rate of the resource species and the birth-growth rate of the consumer (Lawton *et al*. 1975, Beddington *et al*. 1976), (3) all organisms allocate resources acquired (i.e. the *supply, S*) in priority order to egestion, conversion costs, respiration (i.e., the Q_{10} rule in poikilotherms) and growth and reproduction. The physiology of assimilation falls under the rubric of the metabolic pool (Petrusewicz & MacFayden 1970). The biology of biomass acquisition is captured using a ratio-dependent functional response model where the sum of maximal genetic *demand* (*D*) is the major parameter (Gutierrez & Baumgärtner 1984). Success in meeting the assimilation demands is measured by the ratio $0 \leq S/D < 1$ that is always less than unity because consumer search is imperfect. The ratio S/D is used in the model to scale maximal vital rates of species (Gutierrez & Wang 1977, Gutierrez & Baumgärtner 1984).

The dynamics model. Seven functional populations {n = 1,…,7} are used to model the system: bay tree mass (n =1), oleander scale mass and numbers {n = 2, 3 respectively}, *A. chilensis* mass and numbers {4, 5}, and *R. lophanthae* mass and numbers {6, 7}. The mass and number dynamics models for each insect species are linked via aging and age-specific births, deaths and net immigration rates.

The well-tested time invariant distributed maturation time model (Vansickle 1977, Gutierrez *et al*. 1984, Severini *et al*. 1990, DiCola *et al*. 1999) (equation 1) is used to model the dynamics of all functional populations. Ignoring subscripts for number and mass, the dynamics of the i^{th} of k age class (i = 1…k) of each functional population (N) is described by equation 1.

$$\frac{dN_i(t)}{dt} = r_{i-1}(t) - r_i(t) - \mu_i(t)N_i(t) \qquad (1)$$

Aging occurs via flow rates $r_{i\text{-}1}(t)$ from $N_{i\text{-}1}$ to N_i with births from all reproductive females entering as a rate ($r_0(t)$) into the first age class (i = *1*), and deaths at maximum age exit from the last or k^{th} age class. The distribution of developmental times of individuals in a cohort through the delay process in the absence of mortality is described by a gamma distribution with characteristic mean (Δ) and variance (s^2). The parameter k defines the shape of the gamma distribution and may be estimated from laboratory data as $k = \Delta^2/s^2$ (see Severini *et al*. 1990). If k is small, the variability of developmental times is large and *visa-versa*. The age width of an age class is Δ/k and the number (or mass) in any age class may be computed as $N_i(t) = \frac{\Delta}{k} r_i(t)$.

Developmental rates. The rate of developmental of poikilothermic organisms (i.e. the transition time through the delay model) varies with temperature T (i.e. $\Delta(T(t) = \Delta(t))$, but it may also vary with nutrition (food supply/demand) and other environmental variables (Gutierrez 1992, Gutierrez *et al*. 1994).[1] The simplest developmental rate model is the linear or degree-day (*dd*) model in which development accrues above a lower thermal threshold (de Candolle 1855). The lower thresholds for bay tree, olive, oleander scale, *A. chilensis* and *R. lophanthae* using this linear models are 5, 9.1, 11, 8.1 and 10.8°C respectively (Fig. 2a; Pizzamiglio 1985), and the developmental times in *dd* of the insects are summarized in Fig. 2b. In our model, a non-linear function is used to capture the full effects of temperature on the developmental rate of each species (Fig. 2a, Table 1, see appendix).

Age specific mortality. Some species and their life stages may be both consumers and resource. Consumer species have preferences for different resource life stages (Fig. 3) (cf. Pizzamiglio 1985, Cividanes & Gutierrez 1996). Time-varying age-specific mortality may accrue from other causes including net emigration, and the combined effect enters equation 1 as a proportional loss rate ($-\infty < \mu_i(t) < +\infty$). Age specific survivorship of i^{th} age scale from the j^{th} factor (i.e. $lx_{(j)i}(t) = 1 - \mu_{(j)i}(t)$) is the product of all survivorship rates affecting the age class (equation 2). We illustrate the computations for age specific mortality of oleander scale, noting that similar models apply to *A. chilensis* and *R. lophanthae.*

$$lx_i(t) = lx_{(cw)i=cw}(T,t)lx_{(T)i}(t)lx_{(s/d)i}(t)lx_{(\mathrm{Pred})i}(t)lx_{(Para)i}(t)) \qquad (2)$$

The mortality components of equation 2 include the effect of temperature on crawler settling ($\mu_{(cw)i=cw}(T,t)$), temperature ($\mu_{(T)i}(t)$), shortfalls of resource(s) as measured by the supply/demand ratio ($\mu_{(s/d)i}(t)$), predation by *R. lophanthae* ($\mu_{(\mathrm{Pred})i}(t)$), and parasitism by *A. chilensis* ($\mu_{(Para)i}(t)$). Mortality enters equation 1 as $\mu_i(t) = 1 - lx_i(t)$. In mass dynamics models, net mass gains enter as an additional factor ($\mu_{(g)i}(t)$).

Initial conditions. The system dynamics were simulated for Albany, California for the period 1 March 1991 to 15 December 1994, and at 108 locations including Albany for the period 1 January 1995 to 31 December 2005. None of the species has a dormant period, allowing the model to be run continuously across years. Fifty oleander scale crawlers were used as the initial populations at all sites, and daily weather (max-min temperatures, solar radiation (Kcal cm^{-2} d^{-1}, rainfall, percent relative humidity and daily runs of wind (km d^{-1})) from each location was used to run the model (see Gutierrez *et al*. 1984).

[1]Time varying distributed delay models may also be developed where Δ is time varying due to nutrition and other factors are easily implemented.

Table 1. Parameters for the oleander scale system model (data from Pizzamiglio 1985, Cividanes and Gutierrez 1996).

Function	Parameters	Units	Oleander scale	*A. chilensis*	*R. lophanthae* Sex ratio (male : female = 0.45)
Life span		Day-degrees			
Immature time	$\Delta(T_{opt})$	(dd)	1565dd >11ºC	750dd >8.13ºC	575dd >10.81ºC
Delay parameter	k		25	25	25
Rate of development	a	–	5.861	2.139	1.606
$R(T) = cT/(a^{T-T_m} + b^{T_m-T})$	b	–	1.132	1.100	1.104
	c	Rate day^{-1}	0.013	0.39	0.042
	T_m	°C	28.601	32.307	35.334
Scalars for $\phi_{(\mu)}(T)$ & $\phi_{(\psi)}(T)$					
$= 1 - \left[\frac{(T(t) - \theta_{\min} - \theta_{mid})}{\theta_{mid}}\right]^2$	θ_{min}	°C	11	8.13	10.8
	θ_{mid}	°C	10.0	13.5	12.0
Fecundity					
(x= adult age in dd)	$Max/\,dd$	–	0.2	0.36	1.4
	a_1	–	0.0335	0.295	–
$\beta_{\max}(x) = a_1 x / b_1^{\,x}$	b_1	–	1.0047	1.0171	–

Geo-referenced simulation output summarizing log cumulative daily numbers of each species over yearly intervals and across the ecological zones of California favorable for olive growth were mapped using a geographic information system (GIS). The GIS was developed using the free GIS software *GRASS* [2]. A window menu allows selection of geographic regions (e.g. the state), ecological regions and evapo-transpiration zones within the state[3], and the elevations to be used in mapping. A text setup file allows specification of the species to be included in the run, the initial conditions for each, the start and stop dates across years for the simulations, the time interval for reporting and mapping the data, raster grid size for kriging and other factors. Any model meeting the minimal input-output requirements can be added to the GIS by simply loading the executable file for the model. The model was first run for all locations and then data were mapped as yearly summaries (or other interval) using raster-based triangulation kriging methods on a one Km grid, for areas below 750m.[4] Simulation runs across years and regions for all species combinations were run and analyzed using linear multiple regression.

Results

Simulation results. The results for Albany, CA are presented in four parts: (1) the oleander scale alone, (2) oleander scale interacting with *A. chilensis*, (3) the scale interacting with the coccinellid predator *R. lophanthae,* and (4) all three species together. The dry matter dynamics of bay tree are computed but not reported.

Albany, CA

Oleander scale alone. During the period 1 March 1991 to 15 December 1994, 5,044 *dd* above the oleander scale's threshold (11°C) accrued at Albany, Ca. As the scale egg–to-egg period is 796 *dd*, roughly 6.3 overlapping generations developed during the period. In the absence of natural enemies, simulated oleander scale populations per tree increase exponentially into the millions (e.g. $>2x10^6$ small second instar scale, Fig. 4). Despite a longer developmental time, adult densities ($5x10^5$) were lower than those of younger stages due to mortality of immature stages caused by resource supply-demand shortfalls and temperature. The number of white caps (a surrogate for reproduction) fluctuated in concert with mean daily temperature (Fig. 4). Over the period, daily min-max temperatures in the range of 5º - 38ºC occurred at Albany, CA exceeding the lower and upper thresholds of the scale for short periods during winter and summer respectively. The temperatures at Albany did affect the scale but were not limiting because the effects on scale fecundity and survival were transient.

Oleander scale and *A. chilensis.* Introducing the parasitoid into the system resulted in a major reduction in immature scale numbers (roughly $4x10^6 \rightarrow 4x10^3$) and caused the cycles

[2]*GRASS* is a open source GIS software package originally developed by the United State Army Corp of Engineers. The version used is that maintained by the GRASS Development Team, 2006. Geographic Resources Analysis Support System (GRASS) Software. ITC-irst, Trento, Italy. http://grass.itc.it.

[3]California Irrigation Management System (CIMIS) evapo-transpiration zones 3, 4,5, 6, 8,10, 12,, 13, 14, 15, 16 (http//:cimis.water.ca.gov/cimis/infoGenCimisOverview.jsp)

[4]Grid sizes and elevations may be varied.

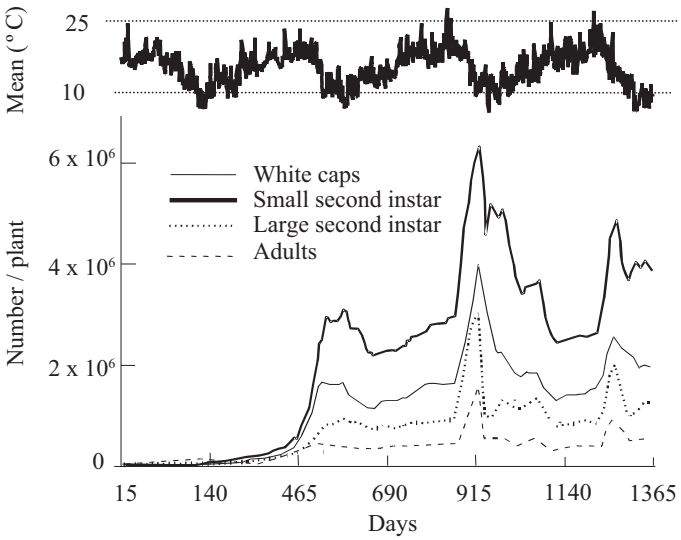

Fig. 4. The simulated population dynamics of oleander scale in the absence of natural enemies using observed weather for Albany, CA from 1 March 1991 to 15 December 1994. Average temperatures are shown in the figure.

of both species to exhibit fairly regular patterns (Fig. 5a). The type III functional response model and emigration of adult parasitoids due to supply-demand shortfalls stabilized model dynamics. A time series plot of late second instar scale density on parasitized scale density (Fig. 5c) illustrates the underlying nature of the regulation of oleander scale by *A. chilensis*[5]. The spiral, albeit left skewed, is characteristic of neutrally stable systems (i.e. limit cycles).

Oleander scale and *R. lophanthae.* Replacing the parasitoid with the coccinellid predator caused scale densities to be reduced a further 50% compared to the action of the parasitoid alone (Figs. 5a vs. 6a). The dynamics of the scale and predator are irregular suggesting periods of predator over-exploitation of prey. A time series plot of late second instar scale density on coccinellid larval density again yields a left skewed, albeit irregular, spiral pattern characteristic of a neutrally stable system (Fig. 6c). The type III functional response of the predator also helps to stabilize the scale-predator system. In addition, when prey densities are low, predator size and hence their demand decline, fecundity drops, and mortality and emigration of adults increase. These effects are caused by resource supply/demand shortfalls that serve to reduce predation pressure.

Oleander scale - parasitoid - predator. Including both natural enemies reduced oleander scale densities a further 30% from that with *R. lophanhae* alone, but it did not greatly changes the irregular pattern of the scale's dynamics (Figs. 6a vs. 7a). The reduction in scale densities is a measure of the parasitoid's added contribution over that of the predator alone, and occurred despite the fact the density of the parasitoid was greatly reduced due to predation and competition (Fig. 7b vs. Fig. 5b). Time series plots of oleander scale density on the density of parasitized scale and on predator larval densities again produced similar left skewed spirals (Fig. 7 vs. Figs. 5-6) suggesting that oscillatory stability is maintained. The similarity of oleander scale dynamics in Fig. 6a vs. 7a and the large suppression of *A. chilensis* densities suggest that the underlying dynamics of the system at Albany CA were largely determined by *R. lophanthae*, thus confirming the findings of Pizzamiglio (1985).

To examine the effects of stochastic temperatures, daily temperatures in the model were allowed to fluctuate daily between 15 to 25ºC, a range of temperatures favorable for the development of all three species. In contrast to the irregular patterns observed using observed weather (Fig. 7a-c), the oscillations of the species become smooth and with defined periods and the average density of the scale is roughly half (Fig. 8a,c). The time series plots of scale density on natural enemy density yield very regular stable limit cycle (Fig. 8d,e vs. Fig. 7d,e). In addition, the left skewness of the scale – *A. chilensis* limit cycles when observed weather was used now become strongly right skewed and suggests a strong response of the parasitoid to increasing host density that is not disrupted by unfavorable temperature (Fig. 8d vs. Fig. 7d). Note that the limit cycles for *R. lophanthae* remain left skewed. Using daily temperature that fluctuated between 10-20ºC further dampened the oscillatory dynamics of the species (results not shown).

Regional GIS simulations. Integrating the model into a GIS allows one to examine the dynamics of the interactions across the olive growing regions of California (Fig. 9). The model for bay tree was replaced in the system by a model for olive (Gutierrez *et al.* 2006), and different combinations of the insect species were run for the period 1 January 1995 to 31

[5]The figure is a time series plot of the scale densities at time t on natural enemy density during the same period.

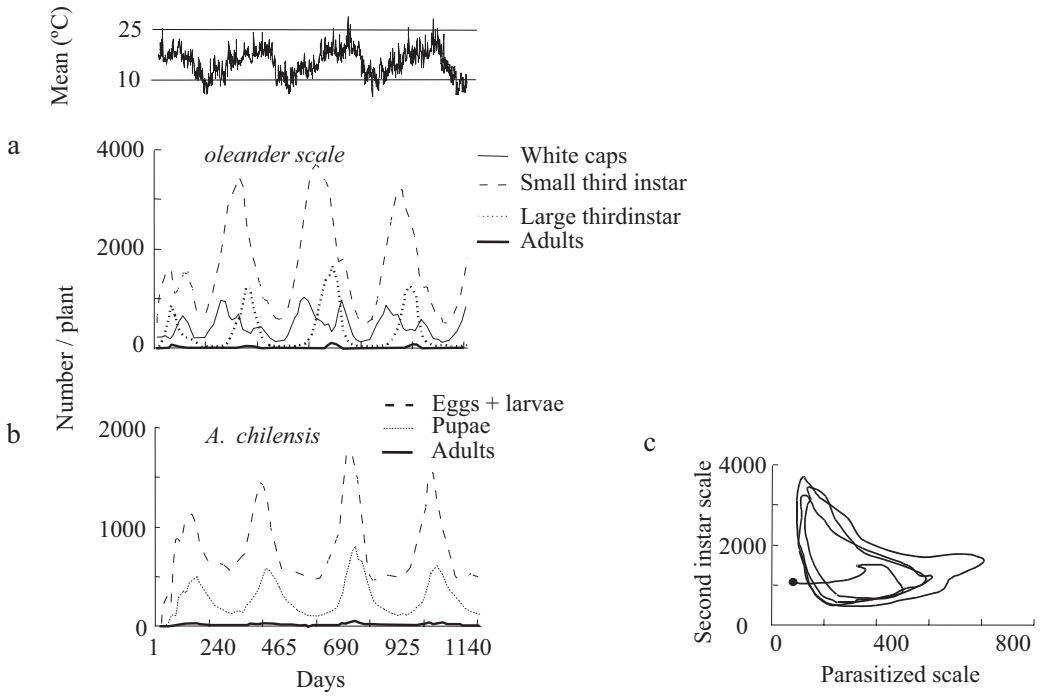

Fig. 5. The simulated population dynamics of (a) oleander scale and (b) the parasitoid *A. chilensis*, and (c) the time series plot of second instar oleander scale on *A. chilensis* parasitized scale. Observed weather for Albany, CA from 1 March 1991 to 15 December 1994 was used in the simulations. Average temperatures are shown in the figure and the symbol ● in subfigure c is the starting points.

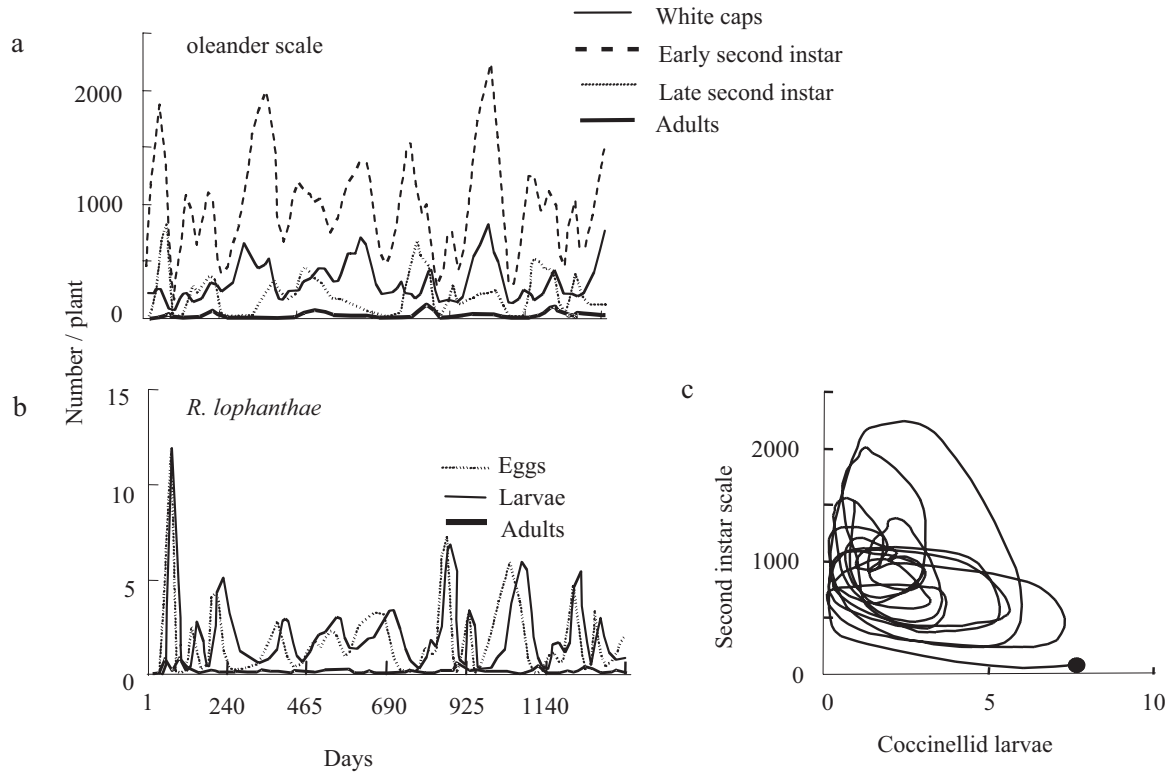

Fig. 6. The simulated population dynamics of (a) the oleander scale, (b) the coccinellid predator *R. lophanthae* using observed weather, and (c) the time series plot of second instar oleander scale on *R. lophanthae* larvae. Observed weather for Albany, CA from 1 March 1991 to 15 December 1994 was used in the simulations. Average temperatures are shown in the figure and the symbol ● in subfigure c is the starting points.

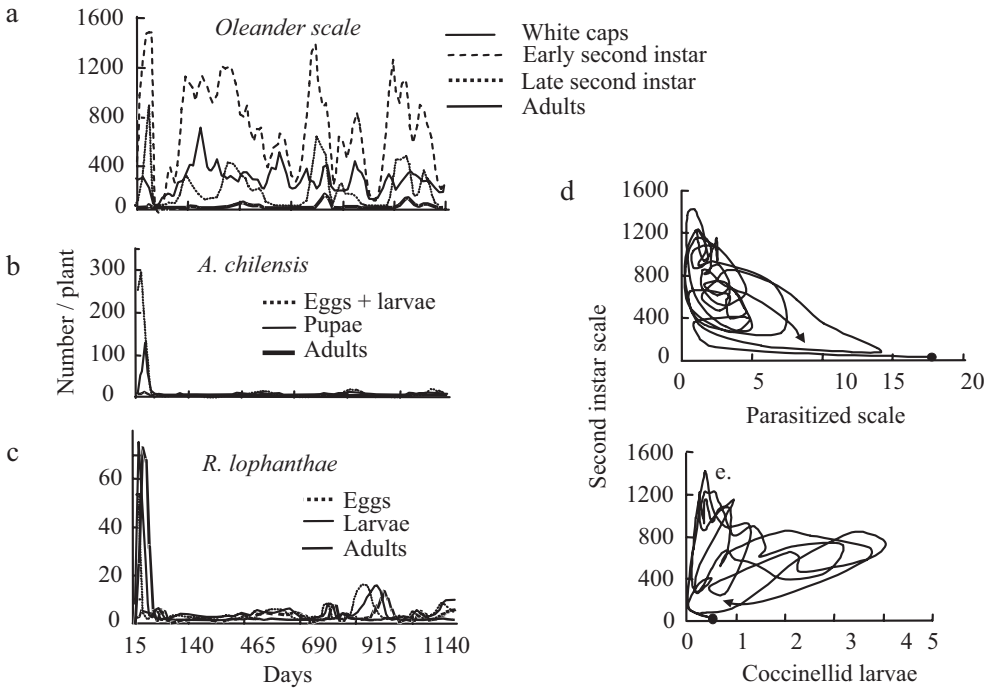

Fig. 7. The simulated population dynamics of (a) the oleander scale, (b) the parasitoid *A. chilensis* and (c) the coccinellid predator *R. lophanthae* using observed weather, and (d, e) the time series plots of second instar oleander scale on *A. chilensis* parasitized scale and *R. lophanthae* larvae respectively. Observed weather for Albany, CA from 1 March 1991 to 15 December 1994 was used in the simulations. Average temperatures are shown in the figure and the symbol ● in subfigures d and e are the starting points.

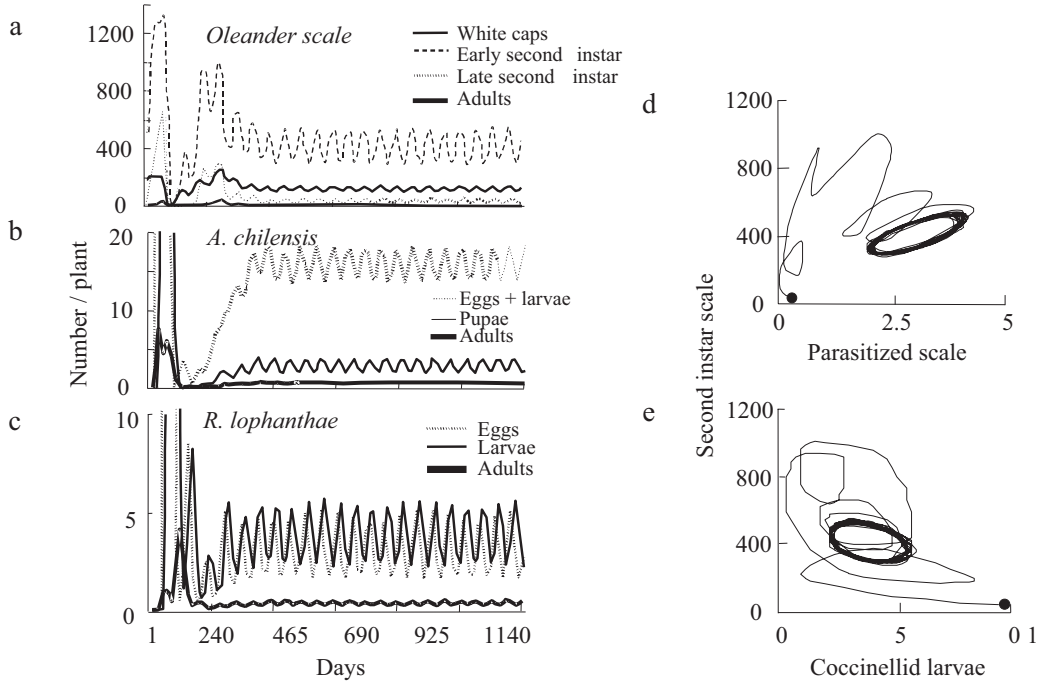

Fig. 8. The simulated population dynamic in a temperature regime that fluctuated daily between 15-25°C: (a) the oleander scale, (b) the coccinellid predator *R. lophanthae* and (c) the parasitoid *A. chilensis* scale and the time series plots of second instar oleander scale on *A. chilensis* parasitized scale (d) and *R. lophanthae* larvae (e). The symbol ● in subfigures d and e are the starting points

December 2005 across all locations. The year-long cumulative daily numbers: of oleander scale larvae plus adults per tree (e.g. scale days), of *A. chilensis* egg-larval stages and of *R. lophanthae* larvae and adults were each computed for each location. The yearly average for each species across years was computed for each location, and of course average daily values may be estimated by dividing by 365 (e.g. $10^{4.5}/365 = 86.6$). GIS maps of the $\log_{10}$ species averages are illustrated in Fig. 9 for the different combinations of species: oleander scale (*Os*), *A. chilensis* (*Ac*) and *R. lophanthae* (*Rl*) (Figs 9a-c); oleander scale - *A. chilensis* (Figs 9d, e); oleander scale and *R. lophanthae* (Fig. 9f, g).

Oleander scale was abundant across all regions of California when both natural enemies were present (Fig. 9a, 10^4 –10^5) but was more numerous in the northern cooler region than in the southern hotter regions. The geographic distribution and abundance of *A. chilensis* is similar to that of oleander scale (9a vs. 9b), while the density of the predator *R. lophanthae* was generally low but most abundant in near coastal areas (9c).

The geographic distribution and abundance of the scale was relatively unchanged when only *A. chilensis* was present (9d, 10^4 –$10^{4.9}$). However, when only *R. lophanthae* was included, scale densities increased generally (e.g. 10^5 –$10^{8.5}$) across all ecological zones (Fig. 9f) with the highest densities occurring in near coastal areas of Central California.

An efficient way to summarize the GIS data across all locations and years is with linear multiple regression analysis. This approach has been used successfully with field and simulation data ((Neuenschwander *et al*. 1989, Gutierrez *et al.* 2005). Here, log cumulative daily oleander scale densities (i.e. $\log_{10}$ *Os*) is used as measures of scale abundance while the length of season in degree-days (*dd*) and dummy variables for the presence-absence (0, 1) of *A. chilensis* (Ac^+) and *R. lophanthae* (Rl^+) and their interactions of the natural enemies are used as independent variables. The goal of the analysis was to estimate the large effects

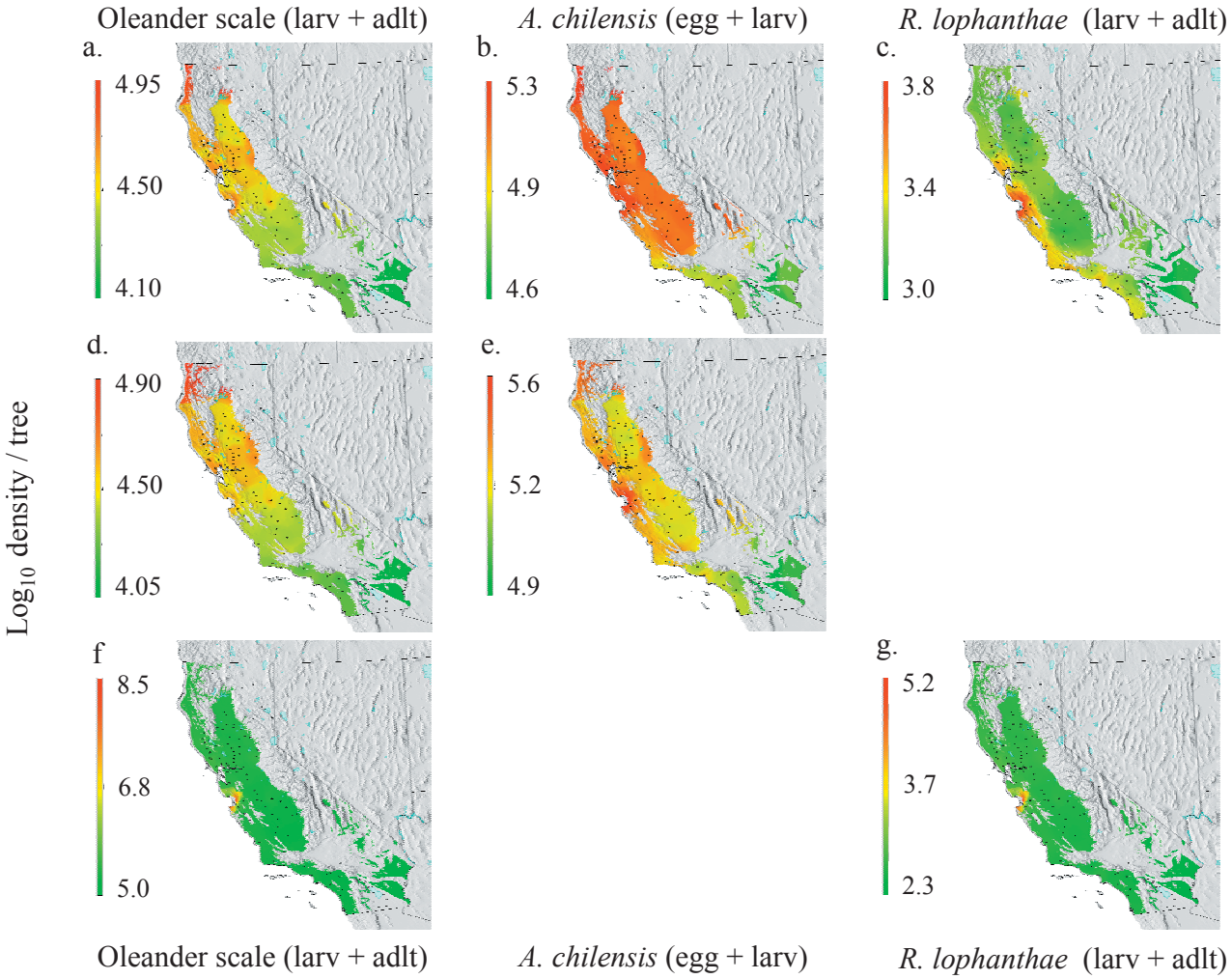

Fig. 9. GIS maps of $\log_{10}$ average yearly cumulative numbers of oleander scale larvae and adults (*Os*), *A. chilensis* eggs and larval stages (*Ac*) and *R. lophanthae* larvae and adults (*Rl*) for period 1995-2005 in the potential olive growing regions of California (i.e. California Irrigation Management Information System (CIMIS) evapo-transparation zones 3, 4, 5, 6, 8, 10, 12, 14, 16 and 16 below 750m elevation; see text for details): (figs. a-c) oleander scale, *A. chilensis*, and *R. lophanthae* respectively; (d, e) oleander scale and *A. chilensis* respectively; (f, g) oleander scale and *R. lophanthae* respectively.

of the independent variables and the interaction $Ac^{+}Rl^{+}$ on scale density and not necessary prediction as measured by R^2. Only those independent variables having slopes significantly greater than zero were retained in the model.

$$\log_{10}Os = 11.66 - 0.101x10^{-2}dd - 5.10Ac^{+} - 4.19Rl^{+} + 4.23Ac^{+}Rl^{+}$$

$$R^2 = 0.949,\ df = 4,015 \text{ and } F = 18,724.2 \qquad (3)$$

The analysis shows that log *Os* decreased with increasing season length (mean annual *dd* across sites = 2103.1 ± 133.3, slope t_{value} = -17.48) and with *A. chilensis* presence (t = -234.2) and *R. lophanthae* presence (t = -192.5). In contrast, the slope of the interaction $Ac^{+}Rl^{+}$ was positive (t = 137.4) and explained 24% of the variance.

Taking the partial derivative $\partial Os/\partial Ac^{+}$ of equation 3 shows that with Rl^{+}=0, the impact of *A. chilensis* is very large being on average 10 fold larger than that of *R. lophanthae* alone. The presence of *R. lophanthae* in the system increases scale density on average by 9.7% (i.e. $10^{-4.19Rl^{+}+4.23Ac^{+}Rl^{+}}$). This result is counter to the field data and simulations from the San Francisco Bay area (Albany, CA) that showed *R. lophanthae* was the more important natural enemy of oleander scale (Pizzamiglio 1985). This reversal is likely due to the fact mild weather conditions are more favorable for *R. lophanthae* (see Fig. 9c, g) that has a short developmental period, attacks parasitized scale and has a high fecundity that enables it to over-exploit prey populations.

Discussion

That abiotic factors limit the distribution and abundance of species and that temperature affects net growth and reproduction in poikilotherms has a long history (von Liebig 1840, Shelford 1931, Andrewartha & Birch 1954, Huffaker et al. 1971). The influence of weather on the control by natural enemies has been posited for the spotted alfalfa aphid [*Therioaphis maculata* (Buckton) (Homoptera: Aphididae)] (Force & Messenger 1964), olive scale [*Parlatoria oleae* (Colvée) (Hemiptera: Diaspididae)] (Huffaker & Kennett 1966), red scale [*Aonidella aurantii* (Maskell) (Hemiptera: Diaspididae)] (Murdoch *et al.* 1996), and others. Weather effects were operative in the classic biological control of the cottony cushion scale [*Icerya purchasi* Maskell (Hemiptera: Margarodidae)] by the vedalia beetle *Rodolia cardinalis* Muls. (Coleoptera: Coccinellidae) in hotter areas, and by the additional action of the parasitic fly *Crytochaetum iceryae* (Will.) (Diptera: Cryptochetidae) in cooler areas (Quezada & DeBach 1973).

What is new is the ability to model these weather driven interactions across ecological zones and the capacity to separate biotic from abiotic effects. The inclusion of weather affects in population dynamics models has a relatively short history (e.g. Hughes & Gilbert 1968, Gilbert & Gutierrez 1973), and the use of physiologically based models has further simplifies the problem (e.g. Gutierrez & Wang 1977, Gutierrez & Baumgärtner 1984, Gurney *et al*. 1996, Gutierrez 1996, Holst *et al*. 1997, Gutierrez *et al*. 2005). Physiologically based demographic models describe basic biological processes of per capita poikilotherm growth and reproduction as driven by weather and as modified by resource density and competition (i.e. inter- and intra-specific). Formulating the models in this manner allows the predictions of the model to be independent of time and place. In this study, we simplified this biology by using physiological indices (e.g., Fitzpatrick & Nix 1970, Gutierrez *et al*. 1974, Sutherst *et al*. 1991) to capture the effects of temperature and resource acquisition success on potential maximal growth, reproduction and survivorship in the oleander scale system (see appendix and Rochat & Gutierrez 2001).

In California, bay tree, olive, the oleander scale and its ectoparasitoid *A. chilensis* and coccinellid predator *R. lophanthae* lack a dormant period and are active throughout the year in areas favorable to their survival. The lower thermal threshold of the oleander scale is high (11°C) and the upper threshold is relatively low (27°C) making its range of favorable temperature relatively narrow compared to those of its natural enemies (Fig. 2). This would tend to restrict the distribution of the scale to Mediterranean climates that are also favorable for olive culture (Fig. 9a). The lower threshold of the parasitoid *A. chilensis* is 8.3°C and its upper threshold is >30°C allowing it to be active during cooler and hotter periods than the scale giving it a wider distribution (Fig. 9b). In addition, the parasitoid's generation time is half that of the scale. The predator *R. lophanthae* has roughly the same lower threshold (10.8°C) as the scale but it has a much higher upper threshold (>35°C) and it generation time is 3/8 that of the scale. Higher levels of abundance of this predator tend to be in the cooler near coastal areas (Fig. 9c).

The field data from the mild climes of Albany, CA in the eastern San Francisco bay area and simulations using weather data from the same location suggested the coccinellid beetle determines the underlying dynamics of the system there because it can rapidly over-exploits parasitized and unparasitized scale populations. Using Albany weather, the simulated densities of oleander scale on bay tree (Fig. 7a) are similar to the low populations reported by Pizzamiglio (1985). This prediction occurs despite the fact that the parameters of the model were estimated independently of the field data. Time series plots of simulated scale densities on natural enemy density suggest that regulation of scale number by both natural enemies is described by a left skewed limit cycle (i.e. plots of resource on consumer), albeit with considerable variability due to stochastic diurnally and seasonally varying temperatures that favor different species at different times. Wide fluctuations in temperature have been shown to increase population fluctuations in the olive-olive scale system (Rochat & Gutierrez 2001).

Field data from Albany, CA indicated the predator *R. lophanthae* was the most important natural enemy suppressing oleander scale (Pizzamiglio 1985), but this proved not to be the case across most of California. Multiple linear regression analysis of the regional simulation data shows that on average, oleander scale densities declined with increasing season length as measured in degree days and with *A. chilensis* presence, but increased 9.7% with *R. lophanthae* presence. This pattern is also seen in the GIS maps of the data (Fig. 9). This conclusion agrees with field observations in the hot dry climate of Greece (Argyriou & Kourmadas 1980) where the parasitoid *A. chilensis* is a more important natural enemy than *R. lophanthae*.

The use of physiologically based demographic models enables analysis of biotic interactions (e.g. prey-predator and others) across a wide range of climatic conditions because the predictions of the model are independent of time and place; they depend on local weather and other factors (Gutierrez & Baumgärtner 1984, Gutierrez 1996). Integrating weather driven models in a GIS provides an excellent way to visualize the data, but an analysis of the simulation data was required to explore subtle biological interactions (e.g. Gutierrez *et al*. 2005). Such physiologically based models are becoming important components in analyses of the effects of climate change on biological systems (Gutierrez *et al*. 2006).

The Dynamics Model

The mathematics and assumptions of the critical components of the model are outlined below and in Gutierrez-Baumgärtner (1984), Gutierrez (1996) and more recently Gutierrez *et al*. (2005).

Population aging with distributed delay. Growth and development of all components were simulated using the Vansickle (1977) distributed maturation time model described here using the notation of DiCola *et al*. (1999, p. 523-524). This model is characterized by the assumption

$$v_i(t) = v(t) = \frac{k}{del(t)}\Delta x \qquad i = 0,1, \ldots,k$$

where k is the number of age intervals and $del(t)$ is the expected value of emergence time and Δx is an increment in age. From (eqn. A1.1) we obtain

$$\frac{dN_i}{dt} = \frac{k}{del(t)}[N_{i-1}(t) - N_i(t)] - \mu_i(t)N_i(t) \quad \text{(A1.1)}$$

where N_i is the density in the ith cohort and $\mu_i(t)$ is the proportional net loss rate. In terms of flux, $r_i(t) = N_i(t)v_i(t)$ yields

$$\frac{d}{dt}\left[\frac{del(t)}{k}r_i(t)\right] = r_{i-1}(t) - r_i(t)] - \frac{del(t)}{k}\mu_i(t)r_i(t) \quad \text{(A1.2)}$$

The model is implemented in discrete form, and observed weather is used to drive the dynamics of the model. Aging and all vital rates are functions of temperature.

Rate of development. In our model, a simple nonlinear model (eqn. A2, Janisch 1925) is used to capture the nature of the relationship more fully noting that we could use other functions as well (e.g. Wellington *et al.* 1999).

$$R(T) = 2c/(a^{T-T_m} + b^{T_m-T}) \quad \text{(A2)}$$

The function $R(T(t))$ is the rate of developmental per day at temperature T, T_m is a threshold, and a, b and c are constants (table 1). The rate of development for oleander scale decrease to zero at about 30°C, while the rates for *A. chilensis* and *R. lophanthae* are still positive at this temperature, but must decline to zero at higher temperatures. The high temperature limits used for *A. chilensis* and *R. lophanthae* are reasonable estimates. In the model, development is completed for each species n when $\sum R_n(T(t)) = 1$.

Resource acquisition. The functional response describes this biology of resource acquisition under different resource and consumer densities and temperature. Here the type II demand-driven ratio-dependent Gutierrez-Baumgärtner (1984) model is used. This model that is a special case of Watt's model (1959, see Gutierrez 1996) where given the appropriate parameters, $f(u)$ (= supply) may be used to compute the resource acquisition rate for any consumer species. Gutierrez (1996) derives the predator and parasitoid forms of this model. To simplify the notation, the subscripts (n) for the consumer are ignored.

$$f(u) = f(R(t), DC(t)) = DC(t)\left[1 - \exp\left(\frac{-\alpha R(t)}{DC(t)}\right)\right] \quad \text{(A3)}$$

C is the density of the consumer population, $D = D(t,T)$ is the maximum per capita consumer demand for resources at time t at temperature T (i.e. the sum of the maximal per capita outflows of the metabolic pool), $D(t,T)C(t)$ is the total population demand, R is the total density of all of the resource populations and □ is the fraction of the resource R available for attack (eqn. A4) and $0 \le \left[1 - \exp\left(\frac{-\alpha R(t)}{DC(t)}\right)\right] < 1$.

Search. However, if α is a concave function of consumer density, this makes eqn. A3 a type III function functional response model with parameters $\alpha_{(0)}$ and s (*cf.*, Rochat & Gutierrez 2001).

$$\alpha(R(t)) = \alpha_{(0)}[1 - \exp(-sC(t))] \quad \text{(A4)}$$

Demand. The total demand $D(t,T)C(t)$ of the consumer population for growth (subscript $\psi = g$) or reproduction ($\psi = f$) varies with age and size (see below), temperature and includes all costs of converting resource to self (eqn. A5).

$$D_\psi C(t) = \sum_{i=1}^{k_n} D_{\psi,i}(T(t))C_i(t) \quad \text{(A5)}$$

Ignoring t, the subscript $i=1 \ldots k$ is consumer age and $D_{\psi,i}(T)$ is the age specific demand for growth (eqn. A6) or reproduction (eqn. A7). Growth demand may be zero in egg, pupa and adult stages and zero for reproduction in immature stages.

Growth For oleander scale and the predator *R. lophanthae,* the per capita age-specific growth demand $D_{\psi,i}(T)$ of its larvae at temperature T may be computed using an exponential growth function (e.g. eqn. A6) on age $x=i$.

$$D_{g,x}(T(t)) = g(T) \cdot m_0 e^{g(T)x} \quad \text{(A6)}$$

The parameter m_0 is the mass of a newly hatched larva, $g(T)$ is maximum consumption rate that includes the costs of egestion, conversion and respiration (see Gutierrez 1996). The demand for reproduction is a fraction of the larval demand at maturity. Parasitized scale may still feed and these demands must also be included.

The percapita demand of adult *A. chilensis* is its age

specific fecundity (i.e. the maximum number of hosts it can attack for oviposition and host feeding at T_{opt}) (eqn. 8, *cf*., Bieri *et al*. 1983).

$$D_{f,x}(T_{opt}) = {c_1 x}\Big/{b_1^x} \quad \text{(A7)}$$

Constants c_1 and b_1 are species specific and were fit to data (Pizzamiglio 1985).

Available resource. Some stages and/or species may be both consumer and resource, hence the density (R(t), number or mass) of all resource species (n) and its sub-stages ($j=1,...,k$) is computed using eqn. A8.

$$R(t) = \sum_{n}^{ns} \sum_{j=1}^{k_n} \xi_{n,j} R_j(t) \quad \text{(A8)}$$

The parameter ($0 \le \xi_{n,j} \le 1$) is the preference of the consumer species for the j^{th} age-stage of the nth resource. Those having preference values equal zero are effectively removed from the calculations (eqn. 9) (Gutierrez-Baumgärtner 1984, Rochat & Gutierrez 2001). These preference functions are depicted in Fig. 3 and were derived from observations reported in Pizzamiglio (1985) and Cividanes & Gutierrez (1996). In all case, the population demand (eqns. A6 or A7) enters the functional response model (eqn. A3) for the n^{th} consumer population (e.g. text Eq. 1).

Assimilation. The biology of biomass assimilation is captured as the net of the acquisition and respiration rates. When plotted on temperature, net assimilation typically yields a concave function over the range favorable for development. The maximum assimilation rate (i.e. growth, reproduction) occurs at the optimum temperature (T_{opt}) with zero values occurring at the upper and lower thermal thresholds. A similar concave relationship is found for survivorship. One can easily derive these relationships from age specific life table data gathered across a range of temperatures and non-limiting resource level (e.g., Force & Messenger 1964, Summers, *et al*. 1984, see Gutierrez 1996). These functions were derived for oleander scale and *A. chilensis* in Pizzamiglio (1985) and for *R. lophanthae* from Cividanes & Gutierrez (1996).

If we normalize these functions, the resulting indices ϕ may be viewed as measures of the temperature related stress the population is experiencing at time t (Gutierrez *et al*. 1994, Rochat & Gutierrez 2001). The physiological indices, $1 \ge \phi_{\psi}(T) \ge 0$, may be captured by a simple, albeit symmetrical, form with subscripts for growth or fecundity ($\psi = g, f$) and survivorship ($\psi = lx = 1-\mu$) (eqn. A9).

$$\phi_{(\psi)}(T) = \begin{cases} 1 - \left(\dfrac{(T - T_{\min}) - \nu}{\nu} \right)^2 & \text{if } T_{\min} \le T \le T_{\max} \\ \text{otherwise } 0 & \end{cases} \quad \text{(A9)}$$

The variables in eqn. 9 are the minimum ($T_{\min}$) and maximum ($T_{\max}$) temperature thresholds for development, and the variable $v = T_{\max} - T_{\min}$ is half the favorable range. The parameters for the three species are summarized in Table 1. To determine the realized growth and/or reproduction rates at temperature T, $f_{\psi}(u)$) (eqn. A3) must be corrected for respiration and cost of converting resource to self, using the temperature growth index ($\phi_{(\psi)}(T)$) (Gutierrez 1992). For example, the realized total population mass birth rate of the consumer population at time t is

$$M_0(t) = \phi_{(f)}(T(t)) f(u) \quad \text{(A10)}$$

with $N_0(t) = M_0(t)/m_0$ being the number eggs produced. Both $N_0(t)$ and $M_0(t)$ enter the first age class of the appropriate species mass or number dynamics equation (i.e. eqn. A1.1). Similarly, the realized growth rates of immature stages of age class i of a consumer are computed as

$$\hat{g}_i(t) = \phi_{(g)}(T(t)) f(u) \frac{D_i(t)}{D(t)} \quad \text{(A11)}$$

$D(T(t))$ is the total population demand (eqn. A7), $D_i(T(t))$ is the demand by the i^{th} age, and $\hat{g}_i(t)$ is its realized growth rate and enters the mass version of text eqn. A1.1 via $\mu_i(t)$ as a proportional increase in mass.

Component Mortality Rates

Mortality may accrue from different factors including resource acquisition shortfalls, predation, parasitism, net immigration and adverse temperatures.

Temperature dependent mortality. Data on the effects of temperature dependent survivorship ($\phi_{(T)}(T(t))$ is normally computed over the life stages of the species, hence the mortality rate of the i^{th} of k age classes is

$$\mu_{(T)i}(t) = \mu_{(T)i}(T(t)) = 1 - \left[\phi_{(\mu)}(T(t))\right]^{1/k} \quad \text{(A12)}$$

In oleander scale, temperature may affect the success rate of scale crawler's ability to settle and feed. For example, success increases as temperatures rises above 9ºC reaching a maximum of about 28 percent above 15ºC (see Pizzamiglio 1985). This is an important source of mortality to newly hatched crawlers of age ($i=cw$) and is captured by eqn. A13.

$$\mu_{(cw)_{i=cw}}(T(t)) = 1 - e^{-0.19(T(t)-9)} \text{ for} \begin{cases} \mathrm{T(t)} > 9^{\circ}C, \\ \textit{zero otherwise} \end{cases} \quad \text{(A13)}$$

The coefficient 0.19 is fitted to data reported in Pizzamiglio (1985).

Mortality due to resource acquisition shortfalls. Shortfall in consumer resource acquisition may increase death rates in feeding non-migratory stages and/or increase migration rates in migratory ones. The mortality or emigration rate of the i^{th} stage of the n^{th} population (subscript ignored) due to resource short falls may be estimated as a function of its supply/demand ratio.

$$0 \le \mu_{(S/D)i}(t) = 1 - \frac{f(C_i(t), R_i(t))}{D_i C_i} = 1 - {\text{supply}}\Big/{\text{demand}} < 1 \quad \text{(A14)}$$

Predation and parasitism. *R. lophanthae* (*Rl*) is a predator of oleander scale (*Ol*) and scale parasitized by *A. chilensis* (*Ac*). The age specific predation rate by *Rl* on resource species *Ol* and *Ac* and their sub-stages of age (*j=1...k*) at time *t* are $\mu_{(Rl)Ol,j}(t)$ and $\mu_{(Rl)Ac,j}(t)$, and with components defined above (e.g. $R_n(t)$, eqn A8) are computed as follows:

$$\mu_{(Rl)Ol,j}(t) = f_{(Rl)n}(u)\xi_{Ol,j}R_{Ol,j}(t)\big/R_n(t) \quad \text{(A15.1)}$$

$$\mu_{(Rl)Ac,j}(t) = f_{(Rl)n}(u)\xi_{Ac,j}R_{Ac,j}(t)\big/R_n(t) \quad \text{(A15.2)}$$

Similarly, the age specific parasitism rate of *Ol* ($\mu_{(Ac)Ol,j}(t)$) sub-stage *j* by *A. chilensis* is

$$\mu_{(Ac)Ol,j}(t) = f_{(Ac)Ol}(u)\xi_{(Ac)Ol,j}R_{(Ac)Ol,j}(t)\big/R_{Ol}(t) \text{ (A16)}$$

Similar models apply to *A. chilensis* and *R. lophanthae.*

Acknowledgments

Special thanks are due Mr. C. K. Ellis for helping to program the model. Weather data was downloaded from the University of California Statewide Integrated Pest Management Program web site (http://www.ipm.ucdavis.edu). The assistance of Dr. Joyce Strand and Mr. Buzz Dryer in obtaining the weather data is much appreciated. The suggestions of an anonymous reviewer were invaluable.

References

Andrewartha, H.G. & L.C. Birch. 1954. The distribution and abundance of animals. The University of Chicago Press, Chicago. 782p.

Argyriou, L.C. & A.L. Kourmadas.1980. The phenology and natural enemies of *Aspidiotus nerii* Bouch`e in Central Greece. Fruits 35: 633-638.

Beddington, J.R., M.P. Hassell & J.H. Lawton. 1976. The components of arthropod predation: II. The predator rate of increase. J. Anim. Ecol. 45: 165-185.

Bieri, M., J. Baumgärtner, G. Bianchi, V. Delucchi & R. Von Arx. 1983. Development and fecundity of pea aphid (*Acyrthosiphon pisum* Harris) as affected by constant temperatures and pea varieties. Mitt. Schweiz. Entomol. Ges. 56:163-171.

Candolle, A. de 1855, Geographic botanique raisonee. Paris, Masson, 606p.

Cividanes, F.J. & A.P. Gutierrez. 1996. Modeling the age-specific per capita growth and reproduction of *Rhizobius lophanthae* (Col.: Coccinellidae). Entomophaga 41: 257-266.

DeBach, P. 1964. Biological control of insect pests and weeds. Chapman & Hall, London, 845p.

DeBach P.& W. Fisher. 1956. Experimental evidence for sibling species in oleander scale, *Aspidiotus hederae* (Vallot). Ann. Entomol. Soc. Am. 49: 235-239.

DiCola, G., G. Gilioli & J. Baumgärtner. 1999. Mathematical models for age-structured population dynamics, p.503-534. In C.B. Huffaker & A.P. Gutierrez (eds.), Ecological entomology. 2nd ed., John Wiley and Sons, New York, 756p.

Ferris, G.F. 1938. Atlas of the scale of North America, Series II. Stanford University Press, California, 137-268p.

Force, D.C. & P.S. Messenger. 1964. Fecundity, reproductive rates, and innate capacity for increase of three parasites of *Therioaphis maculata* (Buckton). Ecology 45: 706-715.

Fitzpatrick, E.A. & H.A. Nix. 1970. The climatic factor in Australian grasslands ecology, p.3-26. In R.M. Moore (ed.), Australian grasslands. Australian National University Press, Canberra, ACT, Australia, 473p.

Gilbert, N.E. & A.P. Gutierrez. 1973. A plant-aphid-parasite relationship. J. Anim. Ecol. 42: 323-340.

Gilbert, N.E., A.P. Gutierrez, B.D. Frazer & R.E. Jones. 1976. Ecological relationships. W.H. Freeman and Co., Reading and San Francisco, 156p.

Godfray, H.C.J. & J.K. Waage. 1991. Predictive modelling in biological control: The mango mealybug (*Rastococcus invadens*) and its parasitoids. J. Appl. Ecol. 23: 434-453.

Gordon, R.D. 1985. The Coccinellidae (Coleoptera) of America North of Mexico. J. N.Y. Entomol. Soc. 93:1-912.

Gurney, W.S.C., D.A.J. Middleton, R.M. Nisbet, E. McCauley, W.W. Murdoch & A. Deroos. 1996. Individual energetics and the equilibrium demography of structured populations. Theor. Pop. Bio. 49:344-368

Gutierrez, A.P. 1992. The physiological basis of ratio dependent theory. Ecology 73: 1552-63.

Gutierrez, A.P. 1996. Applied population ecology: A supply-demand approach. John Wiley and Sons, New York. 300p.

Gutierrez, A.P., D.E. Havenstein, H.A. Nix & P.A. Moore. 1974. The ecology of *Aphis craccivora* Koch and subterranean clover stunt virus. III. A regional perspective of the phenology and migration of the cowpea aphid. J. Appl. Ecol. 11: 21-35.

Gutierrez, A.P. & J.U. Baumgärtner. 1984. Multitrophic level models of predator-prey-energetics: I. Age specific energetics models-pea aphid *Acyrthosiphon pisum* (Harris) (Homoptera: Aphididae) as an example. Can. Entomol. 116: 924-932.

Gutierrez, A.P., L. Ponti, C.K. Ellis & T. d'Oultremont. 2006. Analysis of climate effects on agricultural systems: A report to the Governor of California, California climate change center. http://www.climatechange.ca.gov/climate_action_team/reports/index.html.

Gutierrez, A.P., M.A. Pizzamiglio, W.J. dos Santos, R. Tennyson & A.M. Villacorta. 1984. A general distributed delay time varying life table plant population model: Cotton (*Gossypium Hirsutum* L.) growth and development as an example. Ecol. Model. 26: 231-249.

Gutierrez, A.P., M.J. Pitcairn, C.K. Ellis, N. Carruthers & R. Ghezelbash. 2005. Evaluating biological control of yellow starthistle (*Centaurea solstitialis* L.) in California: A supply-demand model. Biol. Control 34: 115-131.

Gutierrez, A.P., N.J. Mills, S.J. Schreiber & C.K. Ellis. 1994. A physiologically based tritrophic perspective on bottom up - top down regulation of populations. Ecology 75: 2227-2242.

Gutierrez, A.P. & Y. Wang. 1977. Applied population ecology: models for crop production and pest management. In Proc. IIASA Workshop on Pest Management Modelling. Oct. 25-28, Laxenburg, Austria (C.S. Holling and G.A. Norton, eds.).

Holst, N., J.A. Axelsen, J.E. Olesen & P. Ruggle. 1997. Object-oriented implementation of the metabolic pool model. Ecol. Model. 104: 175-187.

Huffaker, C.B. & C.E. Kennett. 1966. Studies of two parasites of the olive scale, *Parlatoria oleae* (Colvée) in control of the olive scale, *Parlatoria oleae* (Colvée). IV. Biological control of *Parlatoria oleae* (Colvée) through the compensatory action of two introduced parasites. Hilgardia 37: 283-334.

Huffaker, C.B., P.S. Messenger & P. DeBach. 1971. The natural enemy component in natural control and the theory of biological control, p.16-67. In C.B. Huffaker (ed.), Biological control. Plenum Press. New York. 844p.

Hughes, R.D. & N. Gilbert. 1968. A model of an aphid population – A general statement. J. Anim. Ecol. 37: 533-563.

Janisch, E. 1925. Uber die Temperaturabhangigkeit Biologischer Vorgange und ihre Kurvenmabige Analyse. Pfluger Archiv fur die Gesamte Physiologie des Menschen und dir tiere 209: 414-436.

Lawton, J.H. 1977. Spokes missing in ecological wheel. Nature 265: 768.

Lawton, J.H., M.P. Hassell & J.R. Beddington. 1975. Prey death rates and rate of increase of arthropod predator populations. Nature 225: 60-62.

Liebig, J. von. 1840. Chemistry and its applications to agriculture and physiology. London, Taylor and Walton. (4th edition 1847).

Murdoch, W.W., C.J. Briggs & R.M. Nisbet. 1996. Competitive displacement and biological control in parasitoids: A model. Amer. Nat. 148: 807-826.

Neuenschwander, P., W.N.O. Hammond, A.P. Gutierrez, A.R. Cudjoe, R. Adjakloe, J.U. Baumgärtner. & U. Regev. 1989. Impact assessment of the biological control of the cassava mealybug, *Phenacoccus manihoti* Matile-Ferrero (Hemiptera: Pseudococcidae), by the introduced parasitoid *Epidinocarsis lopezi* (De Santis) (Hymenoptera: Encyrtidae). Bull. Entomol. Res. 79: 579-594.

Quezada, J.R. & P. DeBach. 1973. Bioecological and population studies of the cottony scale, *Icerya purchasi* Mask. and its natural enemies. *Rodolia cardinalis* Mul. and *Cryptochaetum iceryae* Wil., in southern California. Hilgardia 41:631-688.

Petrusewicz, K. & A. MacFayden. 1970. Productivity of terrestial animals: Principles and methods. IBP Handbook 13. Blackwell, Oxford.

Pizzamiglio, M.A. 1985. Population studies on *Aspidiotus nerii* Bouche (Homoptera: Diaspidae) and two of its natural enemies on California Bay trees. MS Thesis, University of California at Berkeley, 96p.

Rochat, J. & A.P. Gutierrez. 2001. Weather mediated regulation of olive scale by two parasitoids. J. Anim. Ecol. 70: 476-490.

Rosen, P. & P. DeBach. 1979. Species of *Aphytis* of the world (Hymenoptera: Aphelinidae), Series Entomologica, v.17, Israel University Press, Jerusalem, 801p.

Severini, M., J. Baumgärtner & M. Ricci. 1990. Theory and practice of parameter estimation of distributed delay models for insect and plant phenologies, p.674-719. In R. Guzzi, R.A. Navarra & J. Shukla (eds.), Meteorology and environmental sciences. World Scientific and International Publisher, Singapore, 825p.

Shelford, V.E. 1931. Some concepts of bioecology. Ecology 12: 455-467.

Summers, C.G., R.L. Coviello & A.P. Gutierrez. 1984. Influence of constant temperatures on the development and reproduction of *Acyrthosiphon kondoi* (Homoptera: Aphididae). Environ. Entomol. 13: 236-242.

Sutherst, R.W., G.F. Maywald & W. Bottomly. 1991. From CLIMEX to PESKY, a generic expert system for risk assessment. EPPO Bulletin 21: 595-608.

Vansickle, J. 1977. Attrition in distributed delay models. IEEE Trans. Sys., Man. Cybern. 7: 635-638.

Wang, Y. & A.P. Gutierrez. 1980. An assessment of the use of stability analysis in population ecology. J. Anim. Ecol. 49: 435-452.

Watt, K.E.F. 1959. A mathematical model for the effects of densities of attacked and attacking species on the number attacked. Can. Entomol. 91: 129-144.

Wellington, W.G., D.L. Johnson & D.J. Lactin. 1999. Weather and insects, p.313-354. In C.B. Huffaker & A.P. Gutierrez (eds.), Ecological entomology, second edition, John Wiley and Sons, New York, 756p.

Received 25/V/05. Accepted 11/VII/06.